Caffeine; a novel green precursor for synthesis of magnetic $CoFe_2O_4$ nanoparticles and pH-sensitive magnetic alginate beads for drug delivery

Mahnaz Amiri[1, 2], Masoud Salavati-Niasari[*, 1], Abbas Pardakhty[2], Meysam Ahmadi[3], Ahmad Akbari[1]

[1]*Institute of Nano Science and Nano Technology, University of Kashan, P.O. Box 87317-51167, Kashan, Islamic Republic of Iran*

[2]*Pharmaceutics Research Center, Institute of Neuropharmacology, Kerman University of Medical Science, Kerman, Iran*

[3]*Neuroscience Research Center, Institute of Neuropharmacology, Kerman University of Medical Science, Kerman, Iran*

*Correspondence E-mail address: *salavati@kashanu.ac.ir*

Abstract

Hydrogel beads are promising delivery systems for encapsulation and release of drugs due to the mild process of their fabrication from biopolymers. Magnetic $CoFe_2O_4$ nanoparticles (MCFO, 9.72 nm in diameter) were synthesized via a co-precipitation method using caffeine as a new environmentally friendly material in order to alkalinize the medium. Drug-targeting Magnetic beads based on $CoFe_2O_4$ nanoparticles, sodium alginate and chlorpheniramine maleate (CPAM) were synthesized in the presence of Ca^{2+} ions to obtain ionic cross-linked magnetic hydrogel beads. Nanoparticles as well as produced magnetic beads were thoroughly characterized by FTIR, XRD, SEM, nanosizer and VSM techniques. The swelling ratio of beads indicated pH-dependent property with maximum water absorbing at pH 7.4. The in vitro release of beads exhibited significant behavior on the subject of nanoparticles concentration and alginate content. Biocompatibility of the CFO nanoparticles and MCFO/Alg beads are demonstrated through cytotoxicity test via MTT ssaay on U87 cell lines.

Keywords: $CoFe_2O_4$ Nanostructures; Caffeine; Alginate; Magnetic beads; chlorpheniramine maleate; Cytotoxicity.

1. Introduction

Recently, biopolymers have attracted extensively more consideration as raw materials for the preparation of hydrogels owing to their notable properties like biocompatibility, biodegradability, environmental sensitivity, non-toxicity and etc [1–3]. Hydrogels provide a hydrophilic medium in the polymeric network that readily absorbs biological fluids or water without dissolving in [4, 5]. Hydrogels sometimes may absorb from10 to 20% (an arbitrary lower limit) up to thousands of times of their dry weight in water. Due to their significant water content, hydrogels with a soft and elastic 3D structure are very similar to natural tissue, especially soft tissues [6]. Artificial conjugation of hydrogel and inorganic components has received great attention [7, 8] attributable to the synergistic properties between these components that could be considered with tailored mechanical and functional properties and indicated important application in various fields, including enzyme immobilization [9], drug delivery systems [10,11], biomedical applications [12,13], cancer therapy [14]. Different approaches have been used to protect labile drugs from the gastric environment [15]. An interesting method is based on the encapsulation of the drug in alginate by different methods in order to protect the drug from environmental effects or, due to alginate pH dependent solubility, from enzymatic / chemical digestion in gastric fluids [16]. Alginate particles have been employed as carriers for controlled drug release [17, 18]. Sodium alginate contains pendant carboxylate that introduced as a polyanionic copolymer, Physical cross-linking of sodium alginate would be done through electrostatic interactions between aligned glucuronic blocks of alginate chains and polyvalent cations (like Ca^{2+}) [19, 20]. Organic and inorganic nanoparticles [21] including metal nanoparticles [22], clay [23], silica [24], magnetic Fe_3O_4 [25], carbon nanotubes [26] and hydroxyapatite [27] for the synthesis of alginate composite beads with exclusive structure and properties have been used. Among the nanoparticles, Fe_3O_4 with magnetic properties presented into alginate beads widely [28]. Our group tried to introduce $CoFe_2O_4$ (CFO) MNPs that are

eco-friendly synthesized with the increasing emphasis on green chemistry due to the ever growing concern about long-term sustainability [29].It is important to develop environmentally friendly matrix materials for the synthesis of nanocomposites with low temperature and water-based preparation methods especially for the synthesis of inorganic compounds. Cobalt ferrites, among inorganic magnetic materials, have newly become the subject of research concern. CFO MNPs has an inverse spinel structure and it is an significant material that has remarkable magnetic, electrical and optical properties, exploited in various uses, such as catalysis [30], adsorption and separation [31], photonic and electronic devices [32], Ferro fluid technology [33], medical diagnosis [34], drug delivery [35], magnetocytolysis [36], hyperthermia [33], permanent magnets and sensors [34].The model drug used in this context is Chlorpheniraminemaleat (CPAM), 3-(4-chlorophenyl)-N,N-dimethyl-3-pyridin-2-yl-propan-1-amine, an alkyl amine first generation H1-receptor antihistamine, is generally accustomed to treat hay fevers and allergic conditions such as urticarial and rhinitis moreover is an important mediator of various allergic diseases over the years. It is also widely used in small-animal veterinary practices. Chlorpheniramine is of concern for two main details. First, given its high solubility, rapid dissolution, and effective permeability, chlorpheniramine is classified as a Class 1 drug [37, 38]. In consideration of the mentioned concerns, a combination of alginate hydrogel beads with CFO MNPs as a drug carrier is quite desirable and to the best of our knowledge, there is no related reports along with. In the present study, novel alginate/CFO hydro-gel beads (Alg/CFO MNPs) were successfully prepared first by green synthesis of uniform and nanosized grain of CFO MNPs in the presence of caffeine and later formation of alginate hydrogel matrix, besides CPAM loading and release was investigated. The structures of the nanoparticles were characterized using XRD, SEM, FTIR and VSM. The effect of CFO MNPs, Alg and CPAM content of the synthesized beads on the swelling behavior, encapsulation efficiency and drug release were studied. Cytotoxicity effect of various concentrations of MCFO and MCFO/ Alg beads on U87 cell line was investigated by MTT ssaay as well.

2. Experimental

2.1. Materials

Sodium alginate was purchased from Fluka (Switzerland), other chemical reagents like $CaCl_2$ and materials for the synthesis of $CoFe_2O_4$ nanostructures such as $CoCl_2.4H_2O$, $FeCl_3.6H_2O$ and caffeine were commercially available and employed without further purification. Fetal bovine Serum (FBS) and Dulbecco's modified Eagle medium (DMEM) were purchased from Gibco BRL (America). Dimethyl sulfoxide (DMSO) and 3-(4,5-dimethylthiazol-2-yl)-2,5-diphenyl tetrazolium bromide (MTT) were purchased from Sigma (America). The magnetic properties of the samples were detected at room temperature using a vibrating sample magnetometer (VSM, Meghnatis Kavir Kashan Co., Kashan, Iran). Chlorpheniraminemaleat was received as a gift from Kerman pharmaceutics research center.

2.2. Preparation of cobalt ferrite nanoparticles

Cobalt ferrite powder was synthesized via a co- precipitation method, by dissolving $CoCl_2.4H_2O$ and $FeCl_3.6H_2O$ in deionized water in the required mole proportion (1:2) with vigorous stirring for 2 h at 60 °C. Caffeine ($C_8H_{10}N_4O_2$) was used as a base to alkalinize media and added to the mixture of the two salts gradually until the system is solidified. The mixture turned into a dark brown color, indicating the ferrite formation. The precipitate was filtered and washed several times thoroughly with distilled water and then washed with ethanol. After drying for 24 h at 70 °C, an ultrafine powder was obtained. Finally, the samples were placed in an open-air atmosphere that was preheated at 300 °C for thermal treatment. The temperature with steps of 100 °C raised to 500 °C, and the samples were kept at each temperature for 1h.

2.3. Fabrication of magnetic hydrogel beads

Briefly, the desired amount of magnetic CFO powder was dispersed in 50 mL of distilled water and stirred for 1 h then sonicated about 20 min. Sodium alginate was poured into dispersed magnetic CFO solution and allowed to stir overnight until completion of biopolymer dissolving. Thereafter, the final solution was extruded in the form

of droplets through an injector into an aqueous magnetically stirred cross-linking solution 3 wt.% of $CaCl_2$ with stirring speed of 50 rpm. The beads stayed in the solution for 24 h in order to better crosslink. Finally, the beads were filtered and washed several times with distilled water and dried under vacuum for 24 h. In remaining of the manuscript, MCFO/CPAM/Alg means $CoFe_2O_4$ magnetic nanoparticles alginate hydrogel beads whit chlorpheniraminemaleat as drug model. Finally, seven formulations were synthesized by varying amount of CFO nanoparticles, NaAlg and drug content that named CB-2-7 in accordance with Table1. Blank beads synthesized in the presence of no nanoparticles and drug was named CB-1.

2.4. Swelling studies

In order to measure the swelling ratio of synthesized beads, at first 0.1 g of dried beads was immersed in 50 ml phosphate buffer saline (PBS, pH 7.4) and hydrochloric acid buffer (HBS, pH 1.2) separately, at room temperature for 5 h to reach swelling equilibrium. Then, the beads were removed from the media, weighed and the Swelling ratio was calculated using below Equation: Swelling ratio; where Ws and Wd are the weight of the samples swollen in aqueous solutions and in a dry state, respectively. All of the swelling experiments were repeated three times and the mean of results is reported.

2.5. Drug loading and in vitro release

In order to investigate the drug loading and release, chlorpheniramine maleate (CPAM) was selected as a model drug and loaded in CFO/Alg beads. Drug-loaded hydrogel beads were synthesized in the same method as described above except that the sodium alginate aqueous solution contained 50, 75 and 100 mg of CPAM. In order to estimate the drug loading, Encapsulation Efficiency (EE %) and release profile of CFO/ CPM/Alg) was determined using UV–vis spectrophotometer at λmax = 260nm and according to [39, 40]. Encapsulation efficiency (EE %) = weight of Drug in beads /total amount of drug added. For release study, 100 mg of drug-loaded hydrogel magnetic bead was transferred to a dialysis bag (molecular cutoff 12,000) and were dipped in 15

mL buffer solution (pH 1.2 and 7.4) kept at 37 ◦C under a speed constant stirring of 50 rpm. At the Specified time intervals, 2 mL of samples was picked up and using a UV spectrophotometer at λmax260 the quantity of released drug was determined via a standard calibration curve of the drug at different concentrations which standard curve equation is y = 0.0137x +0.0103 (R2 = 0.9995). By replacing 2 mL of the fresh buffered solution instead of taken samples, constant volume was maintained.

2.6. Characterization of samples

The synthesized samples were characterized by a series of technologies involving X-ray diffraction (XRD) patterns that recorded by a Philips-X'pertpro, X-ray diffractometer using Ni-filtered Cu Ka radiation. Fourier transform infrared (FT-IR) spectra were recorded on Nicolet Magna-550 spectrometer in KBr pellets. The electronic spectrum of the sample was taken on Perkin–Elmer LS-55 luminescence spectrometer. Scanning electron microscopy (SEM) images were obtained on LEO-1455VP equipped with an energy dispersive X- ray spectroscopy. The transmission electron microscopy (TEM) image was obtained on a Philips EM208 transmission electron microscope with an accelerating voltage of 200 kV. Uv-vis spectroscopy (diffuse reflectance) of the obtained was performed with a Shimadzu UV/3100 in a range between 200-700 nm. Magnetic properties were measured using a vibrating sample magnetometer (VSM) model of BHV-55, Riken (Japan). An 827 lab pH meter Metrohm, was used for pH measurements. The optical density (MTT assay) was determined at 490nm using a Multiskan MK3 microplate reader (Thermo Fisher Scientific, America).Determination of particle size was done by Master sizer 2000 (England) and Nanosizer cordouan (France).

3. Results and discussion

3.1. Formation of hydrogel networks

The experiment's purpose was to study the effect of various concentrations of CFO MNPs and sodium alginate on drug release of MCFO/Alg/CPAM beads prepared using the extrusion method. Alginate is one of the proper bio-

polymers, which are capable of crosslinking by ionic interactions. Gelled spheres formed instantaneously due to the electrostatic interaction between positively charged Ca ions and negatively charged alginate through the alginate solution was dropped into $CaCl_2$ solution. Fig.1 schematically represents the formation of hydrogel network. In continues of the work CB-4 not only for better appearance, but also because of more MNPs content and drug concentration was chosen for more investigations.

3.2. Fourier transforms infrared spectroscopy

Fig. 2 A Shows the FT-IR spectra of the NaAlg, $CoFe_2O_4$ MNPs, CPAM and their blend MCFO/CPAM/Alg sample (CB-4) respectively. Peaks at 1602, 1425 cm^{-1} indicates the presence of carboxylic acid groups of Alg [41] and peaks at 1584, 1425 cm^{-1} attributed to carboxylic ions of the blend. This shift to the lower wavelength (1602to1584 cm^{-1}) is likely owing to hydrogen bonding of polymer in the blend. Shi et al. [42] detected a new small peak at 1740 cm^{-1} in alginate hydrogel beads, which may occur because of electrostatic interactions between carboxylic groups of alginate and metal ions. The peaks at 3418, 3557 and 3380 cm^{-1} are attributed to OH groups of NaAlg and hydro-gel beads. The FT-IR spectrum of CoFe2O4 supports the formation of spinel structured $CoFe_2O_4$. The typical inverse spinel ferrite structure involves of two IR absorption bands, one at around 400 cm^{-1} which attributes to stretching vibration of tetrahedral groups Fe^{3+} $O^{2-}$and another at around 600 cm^{-1}, representing octahedral group complex Co^{2+} O^{2-} [43]. In the present study the above said bands appear at around 392 and 575 cm^{-1}, respectively, which approves the formation of $CoFe_2O_4$. FTIR spectral data of drug loaded beads in Fig. 2 A were used to confirm the chemical stability of CPAM beads. FTIR spectra of pure CPAM drug and CPAM loaded crosslinked beads were compared. CPAM has shown characteristic bands at 2966 and 2917 cm^{-1} due to aliphatic C-H stretching. The band at 1619 and 1588 cm^{-1} due to C=N stretching vibration. While those of 1476 and 1432 cm^{-1} are due to aromatic C=C stretching vibration. CPAM has also revealed characteristic band at around 864 cm^{-1} due to aromatic C-Cl stretching. When drug was incorporated into the crosslinked alginate /CFO beads, along with all the characteristic band of the crosslinked alginate and CFO,

additional band have appeared as a result of the presence of CPAM in the matrix [44]. It indicates that CPAM has not experienced any chemical change in the form of bead. Furthermore chlorfeniraminemaleat and alginate peaks revealed in CB-4 sample. The presence of alginate can be established by wave number at 1425 cm^{-1} that is attributed to the symmetrical vibration of carboxylate groups on alginate component. Consequently the blend peak proved the synthesis of MCFO/Alg / drug bead.

3.3. XRD analysis

The XRD patterns of the final sample (CB-4) as well as CPAM and MNPs are indicated in Fig. 2B. The presence of (1 1 1), (2 2 0), (3 1 1), (4 0 0), (4 2 2), (5 1 1) and (4 4 0) peaks in the XRD pattern of CFO MNPs (Fig.2B) are in accordance with inverse cubic spinel structure [45].Which is in agreement with JCPDS standard cards no. 01-077-0426 with no extra impurity phases. From the peak of the reflection (3 1 1) of CFO MNPs, we have estimated the particle sizes of the samples Using Sherrer's equation [46], the average size of the MNP crystals were estimated to be 13.2 nm. The crystallinity of the drug in polymeric matrix was analyzed by XRD analysis as well. A crystalline characteristic peak of CPAM drug was observed where as in the case of drug loaded hydrogel beads (CB-4) these sharp peaks were disappeared representing the molecular dispersion of the drug in the polymer matrix [47]. No characteristic XRD pattern was observed in the case of drug-loaded beads. Thus, the X-ray diffraction data of the drug-loaded beads indicates that the drug in the CB-4 sample is in the amorphous state not in the crystalline state. This evidently indicated that during the preparation of the beads by this gelation method, drug crystalline state modification was occurred.

3.4. Morphological investigation

Fig. 3A-C indicates SEM images of $CoFe_2O_4$ sample at different magnifications which agree with the results calculated by the Debye-Sherrer's relation used for estimation of average crystal sizes. The morphology of the magnetic nanostructuress was also studied by TEM that are presented at various magnifications for better

understanding (Fig. 3D-F). The size and typical structure of spheres with narrow size distribution are clearly seen in TEM images, which is consistent with the above-mentioned SEM analysis. Synthesized magnetic nanoparticles because of magnetic interaction were agglomerated strongly. Hence, real size of nanoparticles is not obvious therefore particle size was calculated by Nanosizer cordouan (France) and reported by SBL analyse. In this procedure hydrodynamic radius was omitted as well as it is tried to reduce agglomeration error in order to provide actual size of the particles. The SBL (Statistical Bin Limits) nanosizer histogram of MNPs is reported in Fig. 3 G and the results (Fig. 3H) revealed that the mean particle size is 9.72 ± 0.15 nm in diameter. Reported results indicate that $CoFe_2O_4$ MNPs provide homogenous dispersity and narrow size distribution. SEM micrographs as a valuable method were used to study the surface morphology of magnetic beads. Optical graph of the resulting beads (CB-4) are presented in Fig. 4A. The CFO/CPAM /Alg beads are spherical, fine unique and homogenous gel structure. This could be because of the interfacial interactions between alginate chains and MNPs which could possibly act as inter-molecular cross-linkers. Furthermore the gel homogeneity was conducted by the virtual diffusion rate between the alginate polymer and Ca^{2+} ions into the gelling zone [48].These results indicate a close interaction of the MNPs with the alginate network. A sponge with many tiny pores (dark areas) on the bead surface was obvious (Fig.4B) that the pores resulted from the removal of water between the crosslinked polymer matrices during the freeze-drying process. The Dynamic light scattering measurements (Fig. 4C) represents that the mean particle size diameter of the hydrogel beads (CB-4) are about 1004.2 ± 1.2µm.

3.5. VSM analysis

Fig. 5 exhibits the magnetic hysteresis loops of CFO nanoparticles and the CB-4 magnetic beads respectively. Magnetization changes were recorded versus field up to 10000 Oe at room temperature. The values of the saturated magnetization (Ms) of MCFO sample and CFO/Alg magnetic beads are about 38.3 and 13.4 emu/g respectively that are different from the bulk value of 80.8 emu/g at room temperature for $CoFe_2O_4$ [49]. The high MS in the co-precipitation method is mainly due to small particle sizes and is slightly owing to the high cation

difference between the two sub-lattices. Fewer coercivity values were observed in the presence of beads sample, however, a clear magnetic response is evident and beads can readily be moved and collected by an external magnetic field.

3.6. Swelling behavior

Swelling abilities of gel are important for substance exchange in tissue regeneration because the three-dimension network of gels can absorb nutrients for cell growth from body fluids [50]. In order to investigate the pH sensitivity of the prepared hydrogel beads, the swelling behavior of the CB-1-CB-5 samples was considered in the pH of 1.2 and 7.4. Swelling rises with time, first rapidly and then slowly, reaching a maximum constant swelling. As shown in Fig. 6A. the swelling ratio of all samples at pH 1.2 was lower than those of pH 7.4. In addition, the results show that CFO/Alg/CPAM beads revealed a lower swelling capacity in comparison to the neat Alg hydrogel beads (CB-1). By comparing swelling degree of CB-2-CB-5 it was apparent that swelling degree reduced with increasing MNPs and alginate content. It may be attributed to the formation of rigid and compacted network with higher cross linker (NaAlg) concentration moreover, the role of MNPs as the knot tying functions is significant, which restricts the increasing of polymer chains. The knot tying function of MNPs may be because of the chelation of some amine and hydroxyl groups of the hydrogel networks with nanoparticles. Similar findings were also reported in the literature by various researchers [51, 52].

3.7. Encapsulation efficiency and in vitro release

The calculated encapsulation efficiency of all formulations was indicated in Fig. 6B. It is obvious from the results that encapsulation efficiency (EE%) increased with increasing drug concentration (50–100 mg) vice versa reduction in %EE was observed with increasing CFO MNPs content in synthesized beads [37]. A promising strategy is the encapsulation of biomolecules, growth factors, and drugs in biodegradable polymer matrices for the continuous release over time [53]. Furthermore, the rate of drug release from the alginate beads (CB-3, 6-7) was

compared at different pH values (Fig. 6C). The beads loaded with 100 mg of drug (CB-3) showed slower drug release compared to the formulations loaded with lower drug content (CB-6 and CB-7) [54]. The release profile of samples were higher at neutral pH compared to acidic pH revealed that the diffusion of drug from hydrogels is firmly controlled by the pH of environment. This may be attributed to protonation and deprotonation of carboxylic acids at various pH of environment. Frequently, carboxylic acids undergoes protonation in acidic conditions (pH = 1.2) and controlling the swelling of hydro-gel beads leading to decline in diffusion of the drug [41]. Deprotonation of bead's carboxylic acid groups occur at pH 7.4 due to ionization leading to higher swelling which further lead to greater diffusion of drug through polymeric hydrogel beads [55]. A prolonged release of CB-5 in comparison to CB-3 was observed (Fig. 6D) as a result of the presence of 3% w/v alginate content. This could be attributed to the dense gel structure of beads, possibly reduced the diffusion of Na+ ions into the beads and therefore, delaying the process of ion exchange between Ca^{2+} and Na^{+} causing in a faster degree of cross linking that caused lower release of the beads. The high content of released drug was observed for CB-2 beads (Fig. 6E) with the lowest amount of magnetic nanoparticles and was in agreement with the swelling behavior of hydrogels. It is noticed that decline in cumulative release with increasing CFO MNPs concentration (CB-2-4), probably is because of the formation of stiff and compact polymer network structure thereby decreasing free voids in hydrogel beads, this permits to diminish the penetration of water molecule into polymer matrix leading to decline in diffusion of drug molecules [51].

3.8. Cytotoxicity

To evaluate the biocompatibility of MCFO/Alg beads, an MTT cytotoxicity assay on the U87 cell lines (in a human primary glioblastoma cell line with epithelial morphology) was performed and the corresponding cell viability exhibited in Fig. 7A. Cells were seeded at a density of 10×103 cells per well in 96 well plates. The plate was incubated in a CO_2 incubator at 37 °C for 24 h thereafter different concentrations of MCFO nanoparticles and CFO/Alg beads suspension was added to each well separately and incubated for another 24 h. Concentration

range was selected as 50, 100, 200, 400 and 600 µg/ml. The media were substituted with fresh media besides, 10µL of 5% MTT filtered solution, was added to each well and incubated for 2 h. The cell viability was recorded using the following formula [56]: Cell viability (%) = (Atest /Actrl) ×100; Where Atest and Actrl are the absorbance values of the test and the control well, respectively. As exposed in Fig. 7A, no serious toxicity (>80% cell viability) of MCFO nanoparticles was measured at the lower concentrations (≤400 µg/mL), demonstrating the acceptable biocompatibility of samples. However, a growth inhibition at a higher concentration (600 µg/mL) was investigated, which reveals that CFO MNPs, display concentration-dependent toxicity to U87 cells. The high cell viability of CFO/Alg beads in all concentrations is attributed to the encapsulation of CFO nanoparticles in the bead via ligand exchange method. The optical micrograph of cells incubated with 600 µg/mL of CFO/Alg hydrogel beads is presented in Fig. 7B. Since alginate is the well-known biopolymer for in vivo treatments [57], these stimuli-responsive beads could have potential to be applied in biomedical, pharmaceutical, regenerative medicine and tissue engineering.

4. Conclusion

In this study, novel pH sensitive magnetic beads with controlled drug release property, based on CoFe2O4 nanoparticles were fabricated. MNPs were prepared using a green novel precursor; caffeine. The SEM images, XRD and SLB data showed that the MCFO nanoparticles with average particle size of 9.72 ± 0.15 nm in diameter are dispersed uniformly. Chlorpheniramine maleate was entrapped in calcium alginate beads prepared by the ionotropic gelation method. The physico-chemical properties such as swelling studies, encapsulation efficiency and in vitro release profiles altered on varying the pH and compositions of beads. Drug release was directly proportional to the polymer concentration and CPAM content. Not only the higher dose of the drug are loaded in pH 7.4, but also the drug may be released more gradually over time with a longer duration of action because of trapping the CPAM inside the carbon pores and cavities. Based on these findings besides no cytotoxicity effect of synthesized beads on U87 cell line, the prepared hydrogels can be used in different medical fields.

Acknowledgements

Authors are grateful to the council of Iran National Science Foundation (INSF) and University of Kashan for supporting this work by Grant No (159271/89450).

References

[1] J.K. Oh, D.I. Lee, J.M. Park, Biopolymer-based microgels/nanogels for drug delivery applications, Prog. Polym. Sci. 34 (12) (2009) 1261–1282.

[2] A. Kumari, S.K. Yadav, S.C. Yadav , Biodegradable polymeric nanoparticles based drug delivery systems, Colloids Surf. B Biointerfaces. 75 (1) (2010) 1–18.

[3] S. Barkhordari, M. Yadollahi, H. Namazi, pH sensitive nanocomposite hydrogel beads based on carboxymethyl cellulose/layered double hydroxide as drug delivery systems, J. Polym. Res. 21 (6) (2014) 1–9.

[4] Z. Mohamadnia, M.J. Zohuriaan-Mehr, K. Kabiri, A. Jamshidi, H. Mobedi, Ionically crosslinked carrageenan-alginate hydrogel beads. J. Biomat. Sci.-Polym. E. 22(2007)342–356.

[5] K. Chen, Y. Ling, C. Cao, X. Li, X. Chen, X. Wang, Chitosan derivatives/reduced graphene oxide/alginate beads for small-molecule drug delivery. Mater. Sci. Eng. C. 69 (2016) 1222–1228.

[6] J.M.Yang, et.al. Cell proliferation on PVA/sodiumalginate and PVA/poly(γ-glutamic acid) electrospun fiber. Mater. Sci. Eng.C. 66 (2016) 170-177.

[7] Z.A.C. Schnepp, R.Gonzalez-McQuire, S.Mann, 2006. Hybrid biocomposites based on calcium phosphate mineralization of self-assembled supramolecular hydrogels, Adv. Mater. 18 (2006)1869–1872.

[8] S. M. H. Dabiri , A. Lagazzo, F. Barberis, M. Farokhi, E. Finochio, L. Pastorino, Characterization of alginate-brushite in-situ hydrogel composites. Mater. Sci. Eng.C. 67 (2016) 502–510.

[9] S Dumitriu, E.Chornet, Immobilization of xylanase in chitosan–xanthan hydrogels. Biotechnol. Progr. 13 (1997) 539–545.

[10] P. Matricardi, C. Di-Meo, T. Coviello, WE. Hennink, F. Alhaique, Interpenetrating polymer networks polysaccharide hydrogels for drug delivery and tissue engineering, Adv. Drug Deliver.Rev.65 (2013) 1172–1187.

[11] T.A. Debele, Sh. L. Mekuria, H.-Ch Tsai, Polysaccharide based nanogels in the drug delivery system: Application as the carrier of pharmaceutical agents. Mater. Sci. Eng. C. 68 (2016) 964-981.

[12] G. Leone, R.Barbucci, Polysaccharide Based Hydrogels for Biomedical Applications. In: Barbucci R, editor. Hydrogels. Milan: Springer; 2009. p. 25–41.

[13] Y. Zhang, X. Wang, Y. Su, D. Chen, W. Zhong, A doxorubicin delivery system: Samarium/mesoporous bioactive glass/alginate composite microspheres. Mater. Sci. Eng.C.67 (2016) 205-213.

[14] K.Y. Win, E. Ye, Ch.P. Teng, Sh. Jiang , M.Y. Han, Engineering Polymeric Microparticles as Theranostic Carriers for Selective Delivery and Cancer Therapy. Adv. HEALTHCARE. Mater. 2 (12) (2013) 1571-1575.

[15] H. Bera, Ch.Gaini, S. Kumar, S. Sarkar ,Sh. Boddupalli, S.R. Ippagunt, HPMC-based gastroretentive dual working matrices coated with Ca^{+2} ion crosslinked alginate-fenugreek gum gel membrane. Mater. Sci. Eng.C. 67 (2016) 170–181.

[16] G. Auriemma, T. Mencherini, P. Russo, M. Stigliani, R. P. Aquino & P. DelGaudio, Prilling for the development of multi-particulate colon drug delivery systems: Pectin vs. pectin-alginate beads. Carbohydrate Polymers, 92(1) (2013). 367–373.

[17] F. DeCicco, A. Porta, F. Sansone, R.P. Aquino, P. DelGaudio, Nanospray technology for an in situ gelling nanoparticulate powder as a wound dressing. International Journal of Pharmaceutics 473(1–2) (2014) 30–37.

[18] H. Li, F. Jiang, S. Ye, Y. Wu, K.Zhu, D. Wang, Bioactive apatite incorporated alginate microspheres with sustained drug-delivery for bone regeneration application, Mater. Sci. Eng.C. 62 (2016) 779–786.

[19] I. Liakos, L. Rizzello, I.S. Bayer, P.P Pompa, R. Cingolani, A. Athanassiou, Controlled antiseptic release by alginate polymer films and beads. Carbohydr. Polym.92 (2013)176–183.

[20] E. Çelik, C. Bayram, R. Akçapınar , M. Türk, E. B. Denkbaş, The effect of calcium chloride concentration on alginate/Fmoc-diphenylalanine hydrogel networks. Mater. Sci. Eng.C.66 (2016) 221–229.

[21] Z. Li , E. Ye , David , R. Lakshminarayanan, X.J. Loh, Recent Advances of Using Hybrid Nanocarriers in Remotely Controlled Therapeutic Delivery. Small. 35 (12) (2016) 4782–4806.

[22] E. Ye and X.J. Loh, Polymeric Hydrogels and Nanoparticles: A Merging and Emerging Field AUSTRALIAN JOURNAL OF CHEMISTRY, 66 (9) (2013) 997-1007.

[23] R.I. Iliescu, E. Andronescu, C.D. Ghitulica, G. Voicu, A. Ficai, M. Hoteteu, Montmorillonite alginate nanocomposite as a drug delivery system – incorporation and in vitro release of irinotecan. Int. J. Pharm. 463(2014)184–192.

[24] Z. Cao, Y.He, L.Sun, X.Cao, Preparation of alginate/silica composite beads with in vitro apatite-forming ability. Adv. Mater. Res. 236–238(2011)1889–1892.

[25] S. Brulé, M. Levy, C. Wilhelm, D. Letourneur, F. Gazeau, C. Ménager, C.L. Le, Visage Doxorubicin release triggered by alginate embedded magnetic nanoheaters: a combined therapy. Adv. Mater.23 (2011)787–790.

[26] X. Zhang, Z. Hui, D. Wan, H. Huang, J. Huang, H. Yuan, J. Yu, Alginate microsphere filled with carbon nanotube as drug carrier. Int. J. Biol. Macromol. 47(2010) 389–395.

[27] J. Zhang, Q. Wang, A. Wang, In situ generation of sodium alginate/hydroxyapatite nanocomposite beads as drug-controlled release matrices. Acta Biomater. 6 (2010) 445–454.

[28] S. Benhammouda, N. Adhoum, L. Monser, Synthesis of magnetic alginate beads based on Fe3O4 nanoparticles for the removal of 3-methylindole from aqueous solution using Fenton process.J. Hazard. Mater. 294(2015)128–136.

[29] A. Mubayi, S. Chatterji, P.M. Rai, G. Watal, Evidence based green synthesis of nanoparticles. Adv. Mat. Lett. 3(6) (2012) 519-525.

[30] L. Xing-Hua, X. Cai-Ling, H. Xiang-Hua, Q. Liang,W. Tao, L. Fa-Shen, Synthesis and magnetic properties of nearly monodisperse $CoFe_2O_4$ nanoparticles through a simple hydrothermal condition, Nanoscale Res. Lett. 5(2010)1039–1044.

[31] Y. Xingbin, C. Jiangtao, X. Qunji, M. Philippe, Synthesis and magnetic properties of $CoFe_2O_4$ nanoparticles confined within mesoporous silica, Microporous MesoporousMater.135 (2010)137–142.

[32] Z. Shusen, M. Dongxu, Preparation of $CoFe_2O_4$ nanocrystallites by solvothermal process and its catalytic activity on the thermal decomposition of ammonium perchlorate, J. Nanomater. 2010 (2010)1–5.

[33] A.B. Salunkhe, V.M. Khot, N.D. Thorat, M.R. Phadatare, C.I. Satish, D.S. Dhawale, S.H. Pawar, Polyvinilalcohol functionalized cobalt ferrite nanoparticles for biomedical applications, Appl. Surf. Sci. 264 (2013) 598–604.

[34] J. Unyong, T. Xiaowei, W. Yong, Y. Hong, X. Younan, Superparamagnetic colloids: controlled synthesis and niche applications, Adv.Mater.19 (2007) 33–60.

[35] L. Chao, A.J. Rondinone, Z.J. Zhang, Synthesis of magnetic spinel ferrite $CoFe_2O_4$ nanoparticles from ferric salt and characterization of the size-dependent superparamagnetic properties, Pure Appl.Chem.72(2000) 37–45.

[36] V.L. Calero-DdelC, C. Rinaldi, Synthesis and magnetic characterization of cobalt-substituted ferrite (CoxFe3_xO4) nanoparticles, J. Magn. Magn. Mater. 314(2007)60–67.

[37] Z. Li, P.H. Chang, J.S. Jean, W.T. Jiang, H. Hong, Mechanism of chlorpheniramine adsorption on Ca-montmorillonite Colloids and Surfaces a-Physicochemical and Engineering Aspects, 385 (2011) 213–218.

[38] J.M. Custodio, C.Y. Wu, L.Z. Benet, Predicting drug disposition, absorption/ elimination/ transporter interplay and the role of food on drug absorption, Advanced Drug Delivery Reviews, 60 (2008) 717–733.

[39] P.D. Gaudio et al., Alginate beads as a carrier for omeprazole/SBA-15 inclusion compound: A step towards the development of personalized pediatric dosage forms, Carbohydrate Polymers, 133 (2015) 464–472.

[40] P.R. Sarika, N. R. Jamesa, P.R. Anil kumar, D. K. Raj, Preparation, characterization and biological evaluation of curcumin loaded alginate aldehyde–gelatin nanogels. Mater. Sci. Eng.C. 68 (2016) 251-257.

[41] M. Piyasi, S. Kishor, S. Shweta, P.P. Kundu, Formulation of pH-responsive carboxymethyl chitosan and alginate beads for the oral delivery of insulin, J. Appl. Polym. Sci. 129 (2012)835–845.

[42] X.W. Shi, L.P. Du, L.P. Sun, J.H. Yang, X.H. Wang, X.L. Su, Ionically cross-linked alginate/carboxymethyl chitin beads for oral delivery of protein drugs. Macromol. Biosci. 5(2005) 881–889.

[43] R.D. Waldron, Infrared Spectra of Ferrites, Physical Reviews, 99 (1955) 1727-1735.

[44] M. Rani, A. Agarwal, Y. S. Negi, Characterization and Biodegradation Studies for Interpenetrating Polymeric Network (IPN) of Chitosan-Amino Acid Beads Journal of Biomaterials and Nanobiotechnology, 2011, 2, 71-84

[45] JCPDS data base 22-1086.

[46] L.V. Azaroff, J. Buerger, The powder method in X-ray crystallography Acta Cryst. 11(1958) 753-754.

[47] C.A. Tao, J. Wang, S. Qin, Y. Lv, Y. Long, H. Zhua, Z. Jiang, Fabrication of pH-sensitive graphene oxide–drug supramolecular hydrogels as controlled release systems J.Mater. Chem. 22 (2012) 24856–24861.

[48] G. Skjåk-Bræk, H. Grasdalen, O. Smidsrød, Inhomogeneous polysaccharide ionic gels, Carbohydr. Polym. 10 (1989) 31–54.

[49] L.D. Tung, V. Kolesnichenko, D. Caruntu, N.H. Chou, C.J. O'Connor, L. Spinu, Magnetic properties of ultrafine cobalt ferrite particles, Journal of Applied Physics 93 (2003) 7486–7488.

[50] J. Yan et.al., Injectable alginate/hydroxyapatite gel scaffold combined with gelatin microspheres for drug delivery and bone tissue engineering. Mater. Sci. Eng.C.63 (2016) 274–284.

[51] S. Banerjee, S. Singh, S.S. Bhattacharya, Trivalent ion cross-linked pH sensitive alginate-methyl cellulose blend hydrogel beads from aqueous template. Int. J. Biol. Macromol. 57 (2013) 297–307.

[52] Y.H. Lin, H.F. Liang, C.K. Chung, M.C. Chen, H.W. Sun, Physically crosslinked alginate/N,O-carboxymethyl chitosan hydrogels with calcium for oral delivery of protein drugs. Biomaterials 26 (2005) 2105–2113.

[53] Z. Fereshteha, M. Fathi, A. Bagri, A. R. Boccaccini, Preparation and characterization of aligned porous PCL/zein scaffolds as drug delivery systems via improved unidirectional freeze-drying method. Mater. Sci. Eng.C. 68 (2016) 613-622.

[54] S.G. Kumbar, K.S. Soppimath, T.M. Aminabhavi, Synthesis and characterization of polyacrylamide-grafted chitosan hydrogel microspheres for the controlled release of indomethacin J. Appl. Polym. Sci. 87 (2003) 1525–1536.

[55] B. YerriSwamy, C. Venkata Prasad, C.L.N. Reddy, P. Sudhakara, I.D. Chung, M.C.S. Subha, K. Chowdoji Rao, Preparation of sodium alginate/poly (vinyl alcohol) blend microspheres for controlled release applications. J. Appl. Polym. Sci. 125 (2012) 555–561.

[56] Y. Bao, Y. Pan, N.G. Ping, T.Sahoo, L.Wu, J.Li, L.Li, H. Gan, Chitosan-functionalized graphene oxide as a nanocarrier for drug and gene delivery, Small 7 (2011) 1569–1578.

[57] R. Mahjub, M. Radmehr, F.A. Dorkoosh, S.N. Ostad,M. Rafiee-Tehrani, Lyophilized insulin nanoparticles prepared from quaternized N-aryl derivatives of chitosan as a new strategy for oral delivery of insulin: in vitro, ex vivo and in vivo characterizations, Drug Dev. Ind. Pharm. 40 (2014) 1645–1659.

Table 1. Required amount of initial materials for the preparation of magnetic beads

Code	NaAlg (w / v %)	$CoFe_2O_4$ (w / v %)	Drug (mg)%
CB-1	2	0	0
CB-2	2	1	100
CB-3	2	2	100
CB-4	2	3	100
CB-5	3	2	100
CB-6	2	2	75
CB-7	2	2	50

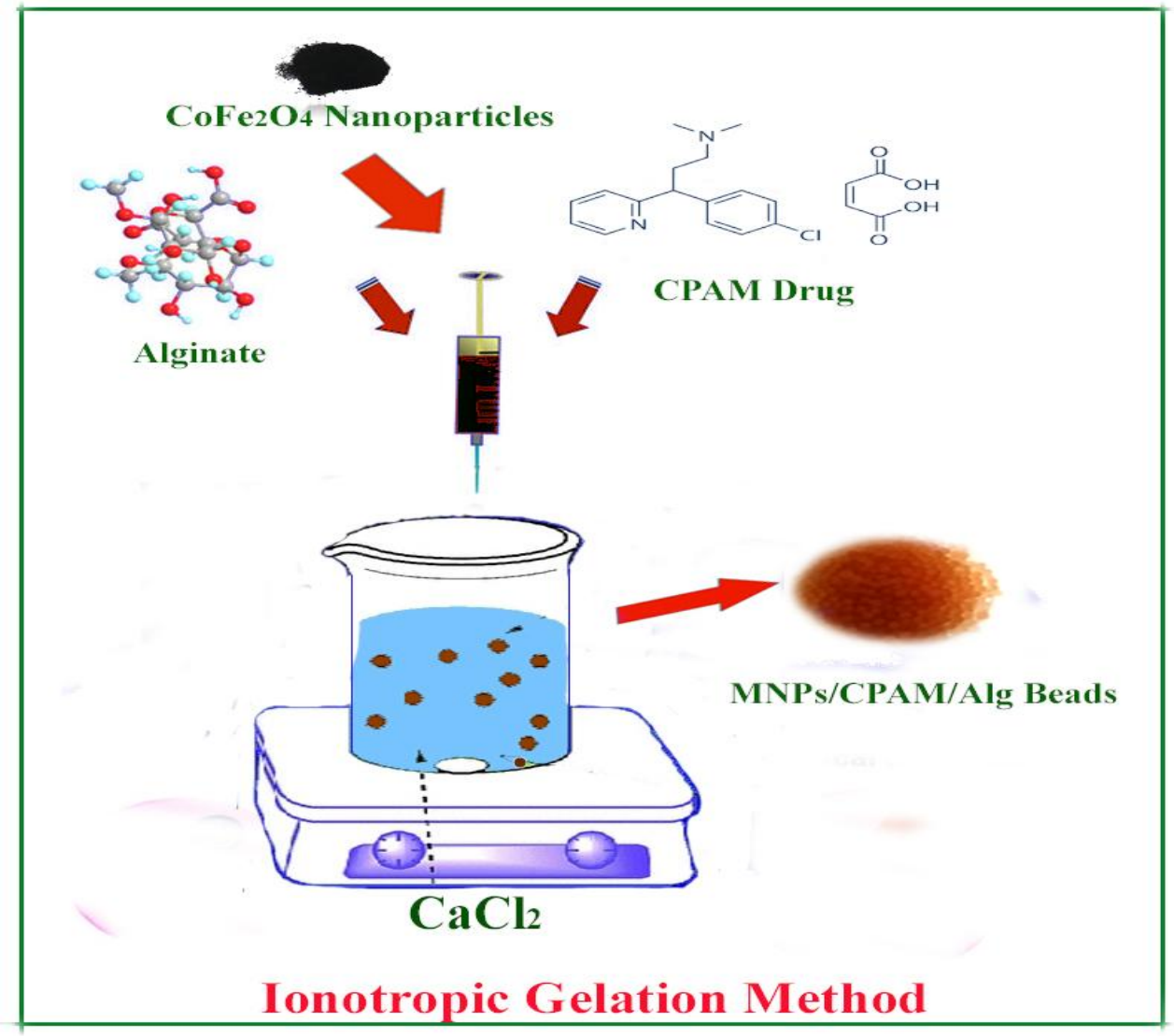

Fig. 1. Schematic illustration of CPAM / MCFO alginate beads preparation

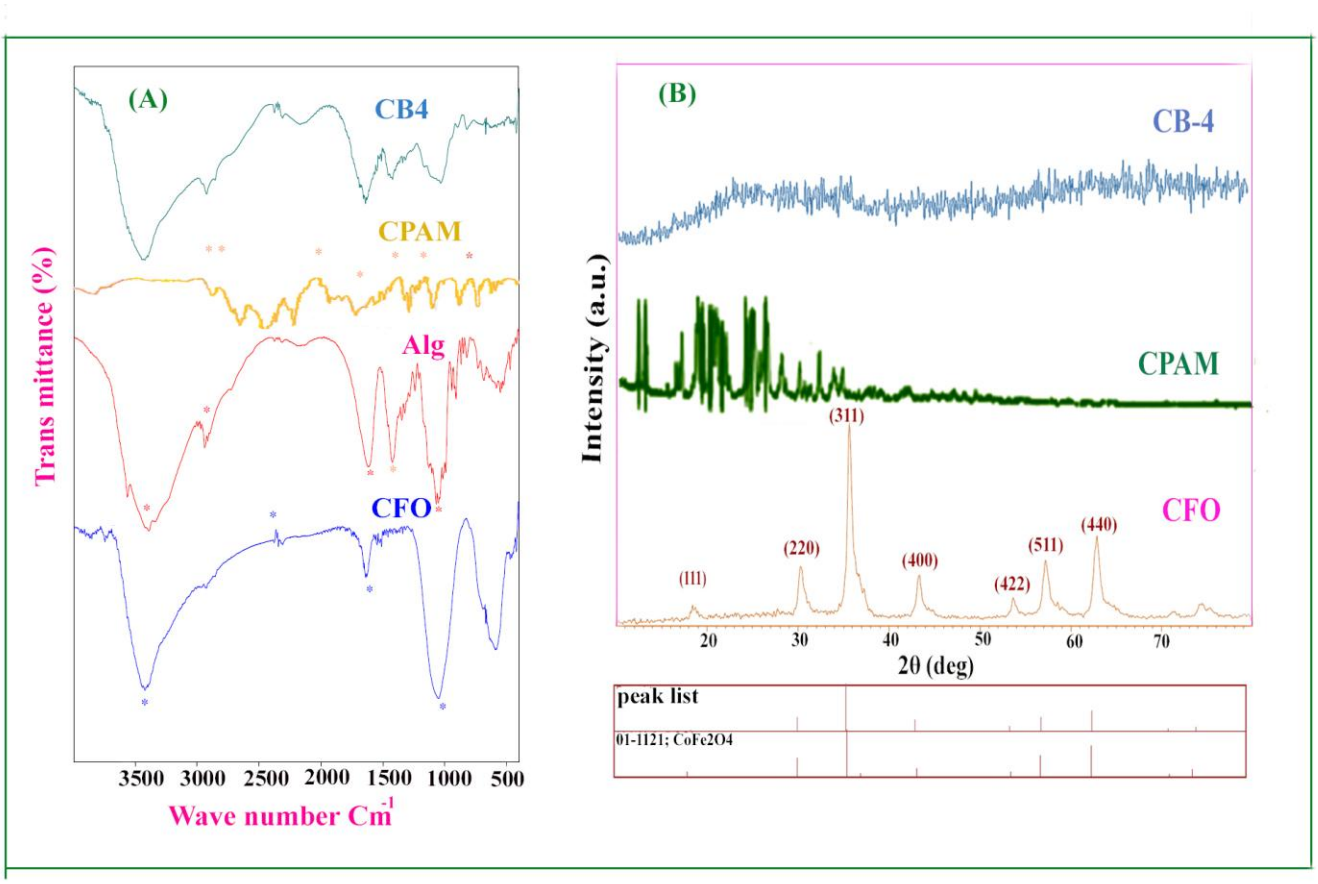

Fig. 2. FTIR spectra of MCFO nanoparticles, alginate, CPAM drug and CB-4 beads sample (A) and XRD patterns of MCFO, CPAM drug and CB-4 beads sample (B).

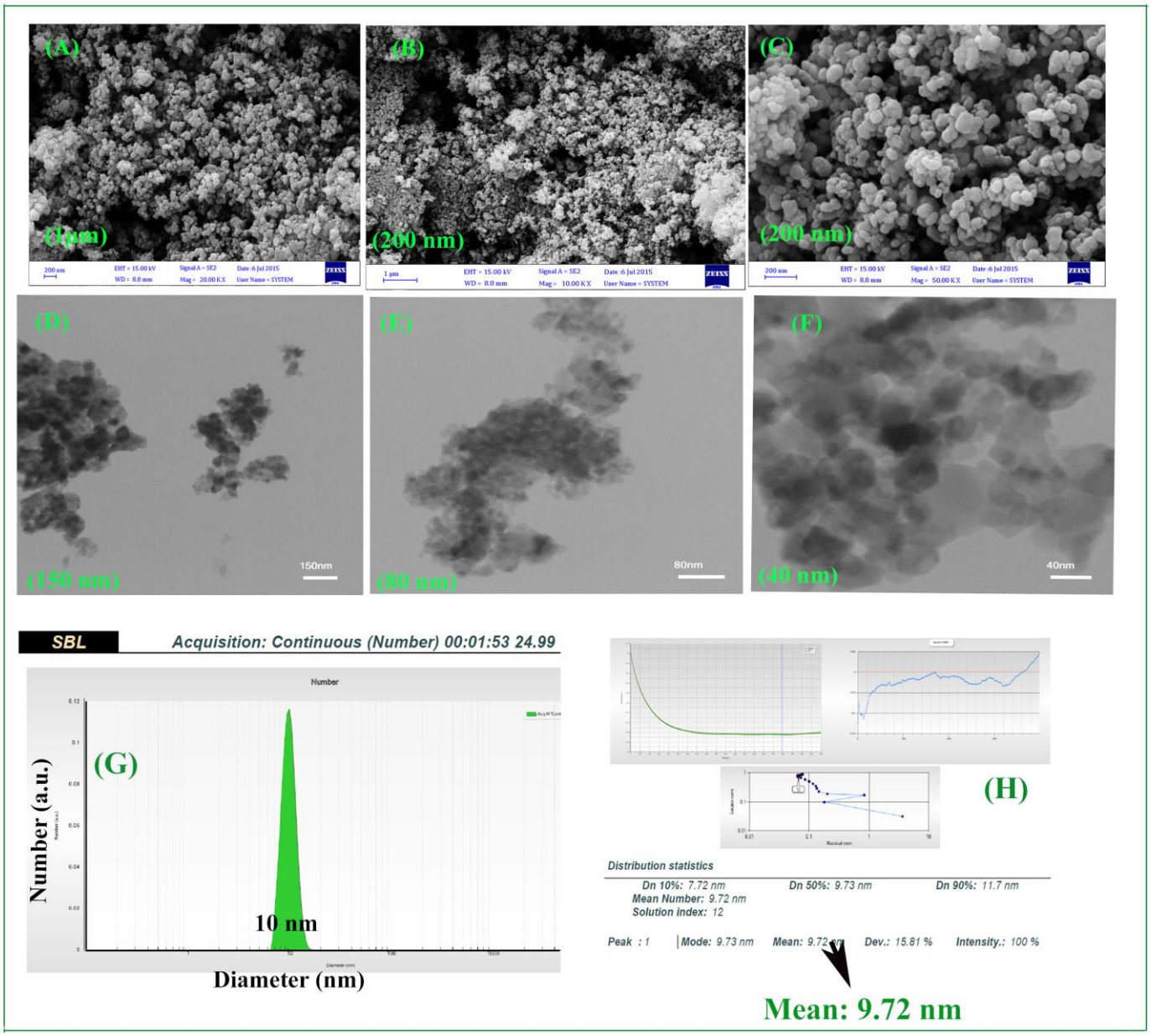

Fig. 3. SEM micrographs of MCFO sample at different magnifications (A) 1µm, (B) 200 nm, (C) 200 nm, TEM micrographs of MCFO sample at different magnifications (D) 150 nm, (E) 80 nm, (F) 40 nm, (G) nanosizer curve of MCFO nanoparticles and (H) SBL report of MCFO diameter in nm.

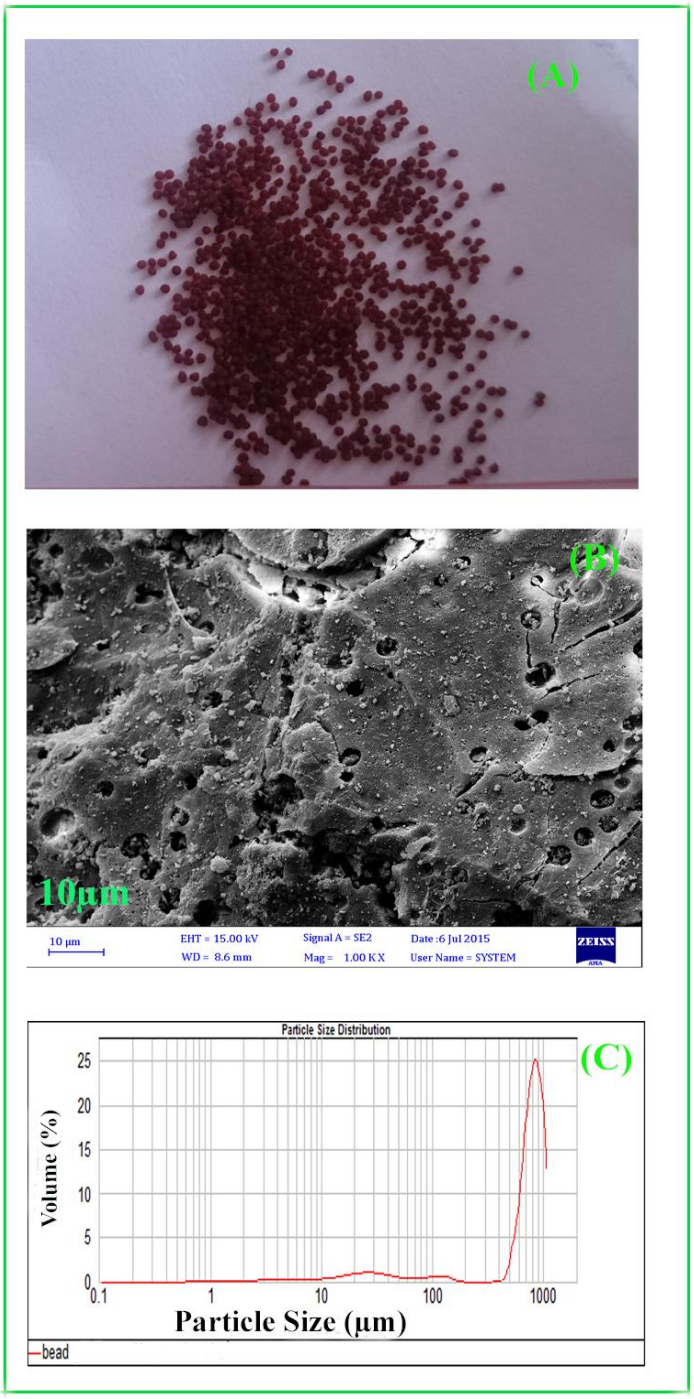

Fig. 4. (A) Optical graph, (B) SEM micrograph of surface and (C) DLS curve of CB4 beads sample.

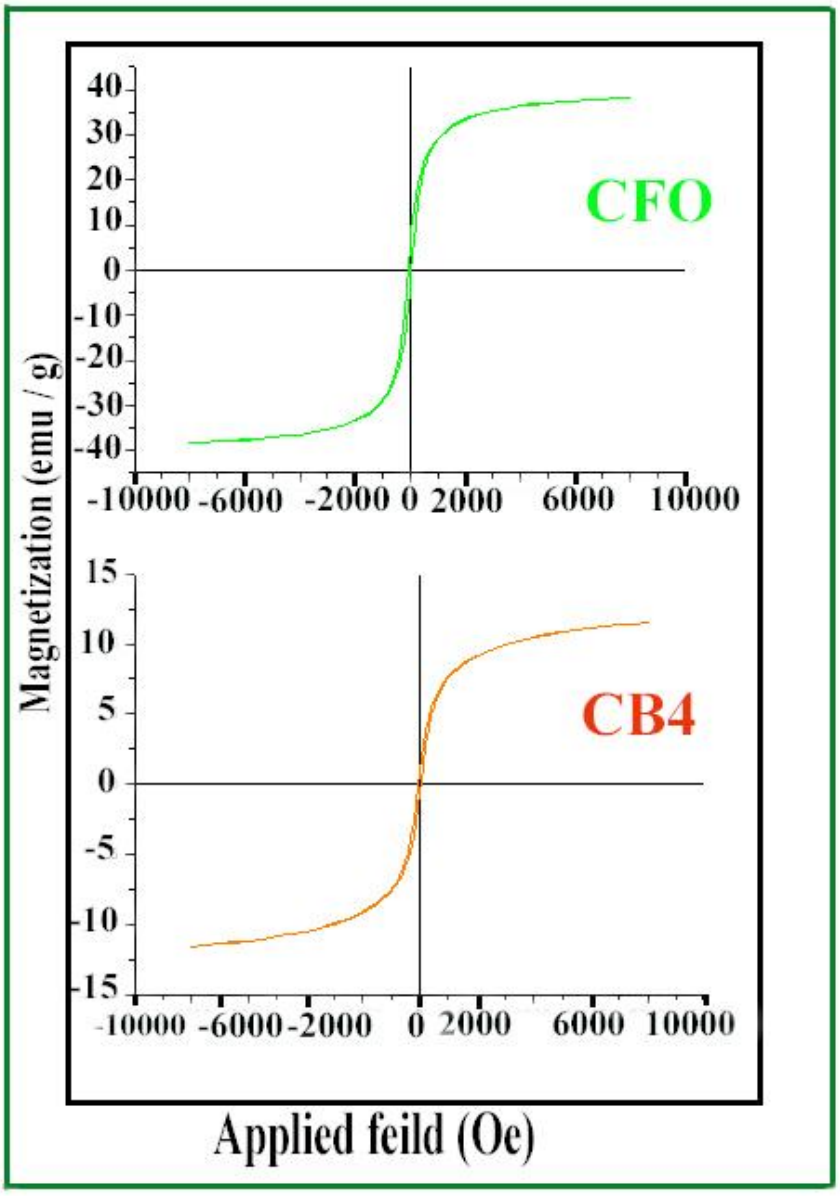

Fig. 5. Magnetic curves of MCFO nanostructures and CB-4 beads product.

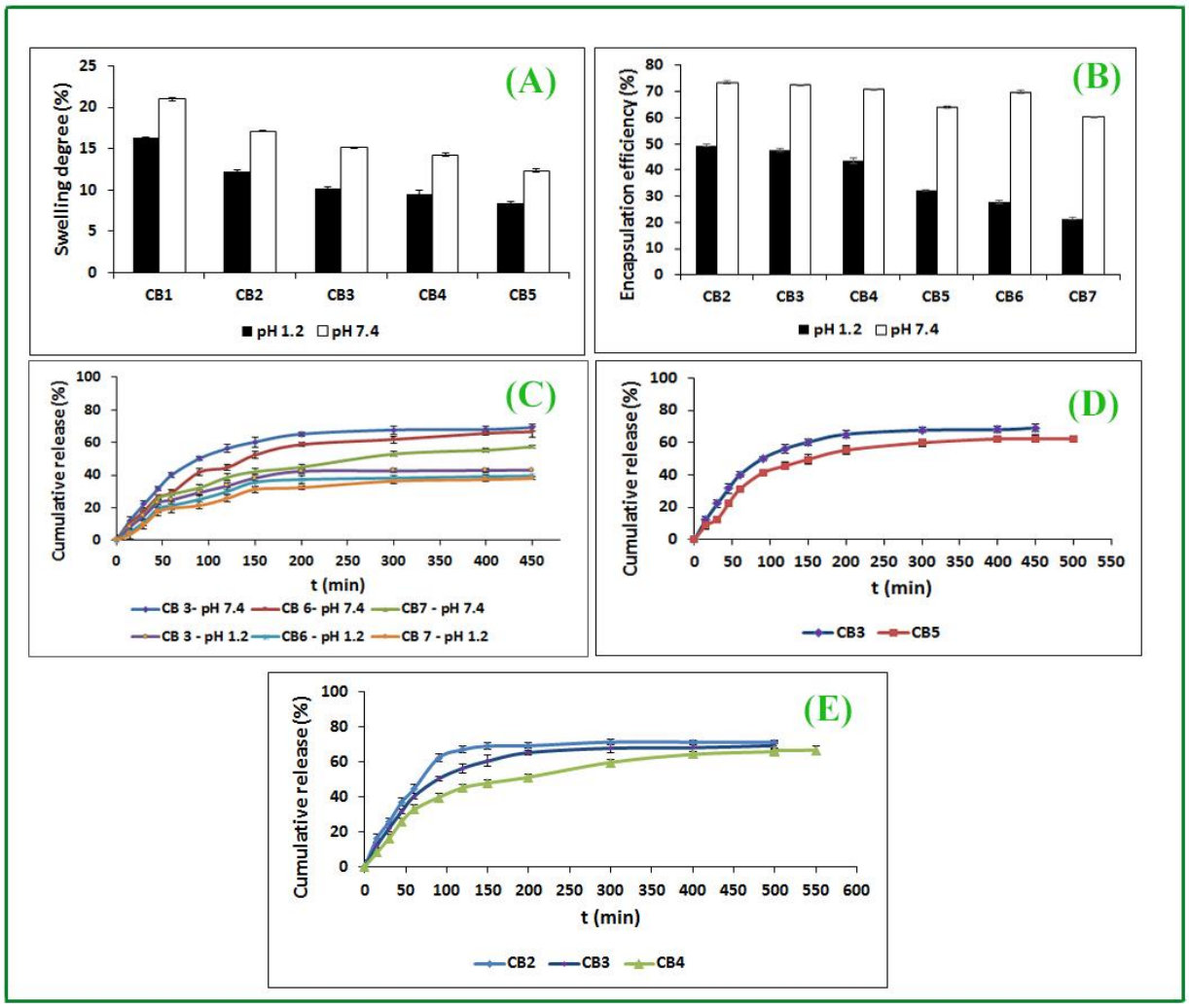

Fig. 6. Effect of pH on Swelling degree (A) and on encapsulation capacity of various beads formulations (B), Investigation of effect of various variables on drug release beads profiles at 37◦C; CPAM drug concentration in various pH (C), alginate content (D) and MCFO content (E).

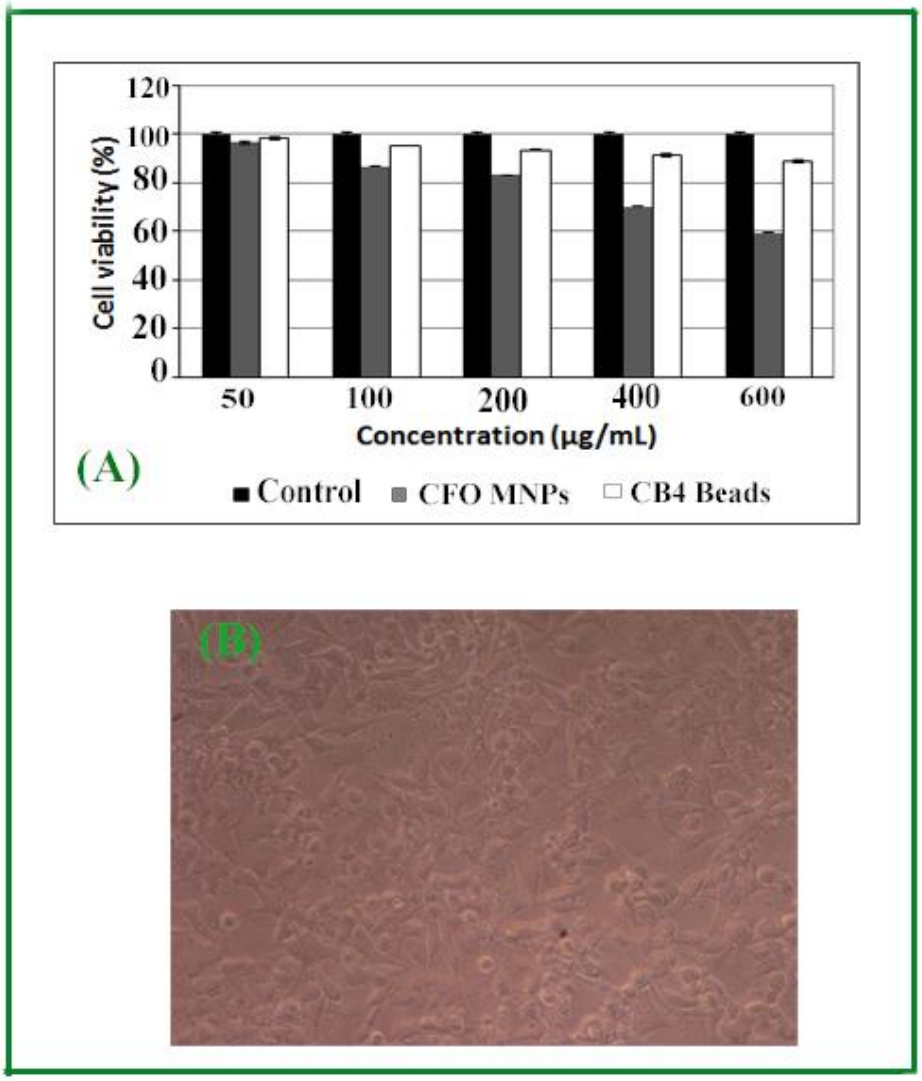

Fig. 7. In vitro cell viability assay and relative optical micrograph. (a) Cell viability of U87 cell lines incubated with MCFO nanostructures and CB-4 beads sample at different concentrations for 24 h (SD ± 2%); (b)Optical micrograph (magnification 200×) of U87 treated with CB-4 beads sample at a concentration of 600 µg/mL.


$C_8H_{10}NO_4$
$CoCl_2$, $FeCl_3$, H_2O
U 87 brain cell
MCFO nanoparticles
MCFO/ CPAM/ Alg beads
Cell viability (%)
150
100
50
0
50
100
200
400
600
Concentration (µg/mL)
Control
CFO MNPs
CB4-bead
Cytotoxicity effect